
EFDA-JET-CP(05)02-40

T.P. Kiviniemi, V. Parail, T. Johnson, J. Lönnroth, T. Kurki-Suonio,
V. Hynönen, J. Heikkinen, S. Sipilä and JET EFDA contributors

Ripple-Induced Fast Ion and Thermal Ion Losses

Ripple-Induced Fast Ion and Thermal Ion Losses

T.P. Kiviniemi¹, V. Parail², T. Johnson³, J. Lönnroth¹, T. Kurki-Suonio¹,
V. Hynönen¹, J. Heikkinen⁴, S. Sipilä¹ and JET EFDA contributors*

¹*Association Euratom-Tekes, Helsinki University of Technology, FIN-02015 HUT, Finland*

²*EURATOM/UKAEA Fusion Association, Oxfordshire, United Kingdom*

³*Association EURATOM-VR, Royal Institute of Technology, Stockholm, Sweden*

⁴*Association Euratom-Tekes, VTT Processes, FIN-02044, VTT, Finland*

** See annex of J. Pamela et al, "Overview of JET Results",*

(Proc.20th IAEA Fusion Energy Conference, Vilamoura, Portugal (2004)).

Preprint of Paper to be submitted for publication in Proceedings of the
EPS Conference,

(Tarragona, Spain 27th June - 1st July 2005)

"This document is intended for publication in the open literature. It is made available on the understanding that it may not be further circulated and extracts or references may not be published prior to publication of the original when applicable, or without the consent of the Publications Officer, EFDA, Culham Science Centre, Abingdon, Oxon, OX14 3DB, UK."

"Enquiries about Copyright and reproduction should be addressed to the Publications Officer, EFDA, Culham Science Centre, Abingdon, Oxon, OX14 3DB, UK."

INTRODUCTION

The magnetic ripple due to the finite number of toroidal coils can significantly affect the behavior and confinement of both thermal and fast ions. In high performance plasmas the ripple-induced losses may significantly enhance the loads on material surfaces. This enhancement has already been analyzed for JET using the Monte Carlo orbit-following code ASCOT [1], but since in normal operation the level of ripple is low in JET ($\delta \leq 2 \times 10^{-3}$), the effect was found insignificant.

A recent proposal to mitigate ELMs with the help of ripple-induced transport [2] has revived the interest in the ripple effects. JET has the unique possibility of controlling the strength of the toroidal ripple, and experiments with varying ripple strength would certainly shed more light on the confinement of ions trapped in the local magnetic mirrors. Therefore it is of interest to repeat the ASCOT simulation with enhanced ripple. ASCOT results can provide a reliable model for the ripple-enhanced transport to be used by the transport code JETTO. The ripple model in ASCOT [4] has now been updated to 3D. With the new model, a much more realistic estimate for the ion losses is obtained, together with the level and localisation of the losses as a function of the ripple amplitude, plasma parameters, and the magnetic configuration.

In this paper the effect of a toroidal ripple is investigated for thermal ions. The ripple effects on fast ions are presented in Ref [5]. Different methods for evaluating heat diffusion coefficient χ_i from Monte Carlo simulation are discussed.

1. ASCOT SIMULATIONS

In ASCOT, each test particle is followed along its guiding-centre orbit determined by the $\vec{E}_r \times \vec{B}$, polarization, gradient and curvature drifts, and collisions. Here, collisions are modelled against a fixed plasma background. In a "pulse spreading simulation" the ion ensemble is initialized at a single flux surface with a Maxwellian velocity defined by the local temperature. In a "full simulation", the test ions are distributed also radially according to the assumed background density profile. This allows obtaining quantitative estimates for the heat loads etc. In the full simulations the density profile is maintained by a radial electric field E_r evaluated from the zero radial ion current density condition as explained in Ref. [4].

The ripple field is given by a JET-based code which calculates the toroidal magnetic field as $B = B_0 + B_1 \cos(16\phi) + B_2 \cos(32\phi)$, where $B_n = B_n(R, Z)$. Here, $B_1 \propto I_1 - I_2$ and $B_2 \propto I_1 + I_2$ are given as a function of different coil currents I_1 and I_2 . In normal JET operation all of the 32 toroidal field coils have the same current I_1 but, to enhance the ripple, we can have two sets of 16 coils, shifted by $p=16$ in toroidal direction, and vary the current I_2 every second coil ($I_2=0$ thus corresponds to a tokamak with only 16 coils). An interface to this data has been programmed into ASCOT, thus upgrading the model to 3D.

2. METHODS FOR CALCULATING TRANSPORT COEFFICIENTS

Two different methods to evaluate ion transport coefficients χ_i from the Monte Carlo simulation are used: In the pulse spreading simulations, χ_i is measured from the variance growth of an initially

radially localized particle ensemble. In the full simulations, the particle ensemble is followed in the presence of collisions and χ_i is estimated from the heat flux measured from the particle ensemble [3].

In the first method, transport coefficient χ_i is evaluated from the spreading of a “pulse”, $f(t=0, r, v) = \Delta(r - r_0) f_M(v)$. If the process is diffusive, the variance will grow at a constant rate $\langle (r(t, v) - r_0)^2 \rangle = V(t, v) = 2D_v(v)t$. Since the flow is proportional to the diffusion coefficient D_v , the transport coefficients are given by

$$\chi_n = \int d^3v (1/2) (dV/dt) (mv^2/2T - 5/2)^n f_M(v); \quad (1)$$

where χ_0 relates pressure gradients to particles transport, χ_1 is the off-diagonal coefficient, and χ_2 relates temperature gradients to energy transport. This technique has been tested against analytic theory with satisfactory agreement. Figure 1(a) displays χ_2 values calculated for the JET Pulse No: 60856 for different ripple strengths and impurity concentrations. There an increase of transport coefficients with a growing ripple was also clearly seen. Simulation with ripple map from JT-60U, which has strong ripple due to only 18 coils, show also strong effect. These results are further confirmed in Figure 1(b), where the heat flux from the full distribution run is evaluated indicating a clear increase in the flux as the ripple is increased.

3. DISTRIBUTION OF LOSSES

The poloidal distribution of ripple losses as a function of the ripple strength is shown in Fig.2 for the pulse spreading simulations. Here, to get qualitative picture, 14400 test particles were initialized at $\rho = 0.97$ and followed over 2ms (collisional time). Background was assumed to have a constant density of $n = 10^{19} \text{ m}^{-3}$ and temperature of $T = 1 \text{ keV}$. The area in which particles are lost to the wall gets wider in the poloidal angle when the ripple increases. It is also of interest to look at the toroidal distribution of the losses. Figure 3, shows the losses to the wall from this same simulation as a function of toroidal angle taking the modulo to one coil period $0 < \phi < 2\pi / 16$. The losses get clearly localized when the ripple increases. However, the divertor losses, do not display clear toroidal structure. From the test particle ensemble even in the highest ripple case no more than about 20% particles go to the wall instead of divertor plates but this fraction depends strongly on simulation parameters. In the full distribution simulations the results are qualitatively the same as for the pulse spreading runs: most of the particles are lost to the divertor, but losses to the wall increase as the ripple increases. Also, fraction of particles going to the wall instead of divertor was observed to increase when temperature increases. Indeed, a similar analysis for fast particles, carried out for ASDEX Upgrade geometry, gives a completely opposite picture: Most of the fast particles are lost to the wall instead of the divertor target, and a clear localisation of particles in the toroidal angle is observed also for divertor losses [5]. Detailed guiding-centre simulations of ion orbit loss heat loads on JET divertor targets has also been performed [6] but there the effect of the ripple was not included.

CONCLUSIONS

Increasing ripple by reducing coil current in every second coil showed clear increase in heat transport in the simulations. The ripple was also found to affect the toroidal distribution as well as the level of losses to the wall: the wall losses got much more local as the ripple increased. It is important to note that this study only included the neoclassical effects arising from guiding centre motion in the presence of collisions. Thus anomalous transport and MHD phenomena are not included. However, the present results can be used as input to the predictive transport models where they may influence the ELM behaviour as shown in Ref. [2]. In return, the ELMs can affect both the level and distribution of heat and particle losses on the wall and the divertor plates.

ACKNOWLEDGEMENTS

The computing facilities of CSC – Scientific Computing Ltd. were used in this work.

REFERENCES

- [1]. T.Kurki-Suonio et al., Nucl. Fusion **42** (2002) 725
- [2]. V. Parail et al., O2.008, this conference.
- [3]. T.P. Kiviniemi et al., Contrib. Plasma Physics **42** (2002) 236
- [4]. J.A. Heikkinen et al., J of Comput Phys **173** (2001) 527
- [5]. T. Kurki-Suonio et al, P4.055, these proceedings
- [6]. S. Sipilä et al, P2.111, these proceedings

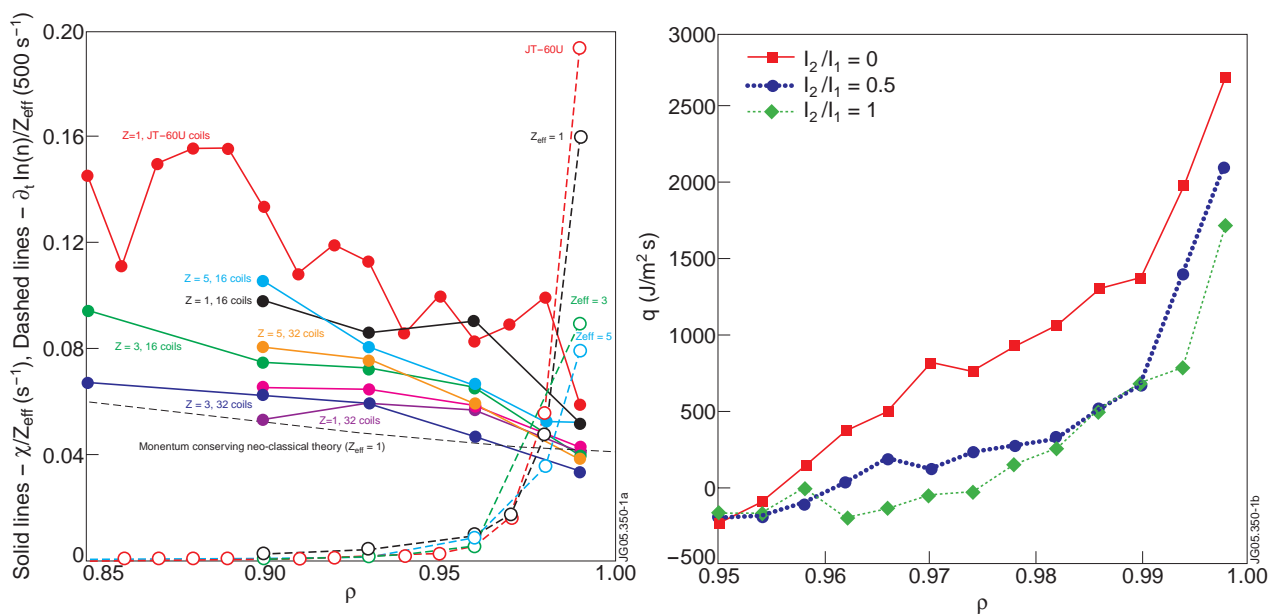


Figure 1: a) Thermal conductivity using pulse-spreading technique and b) heat flux from full simulation and for different values of ripple.

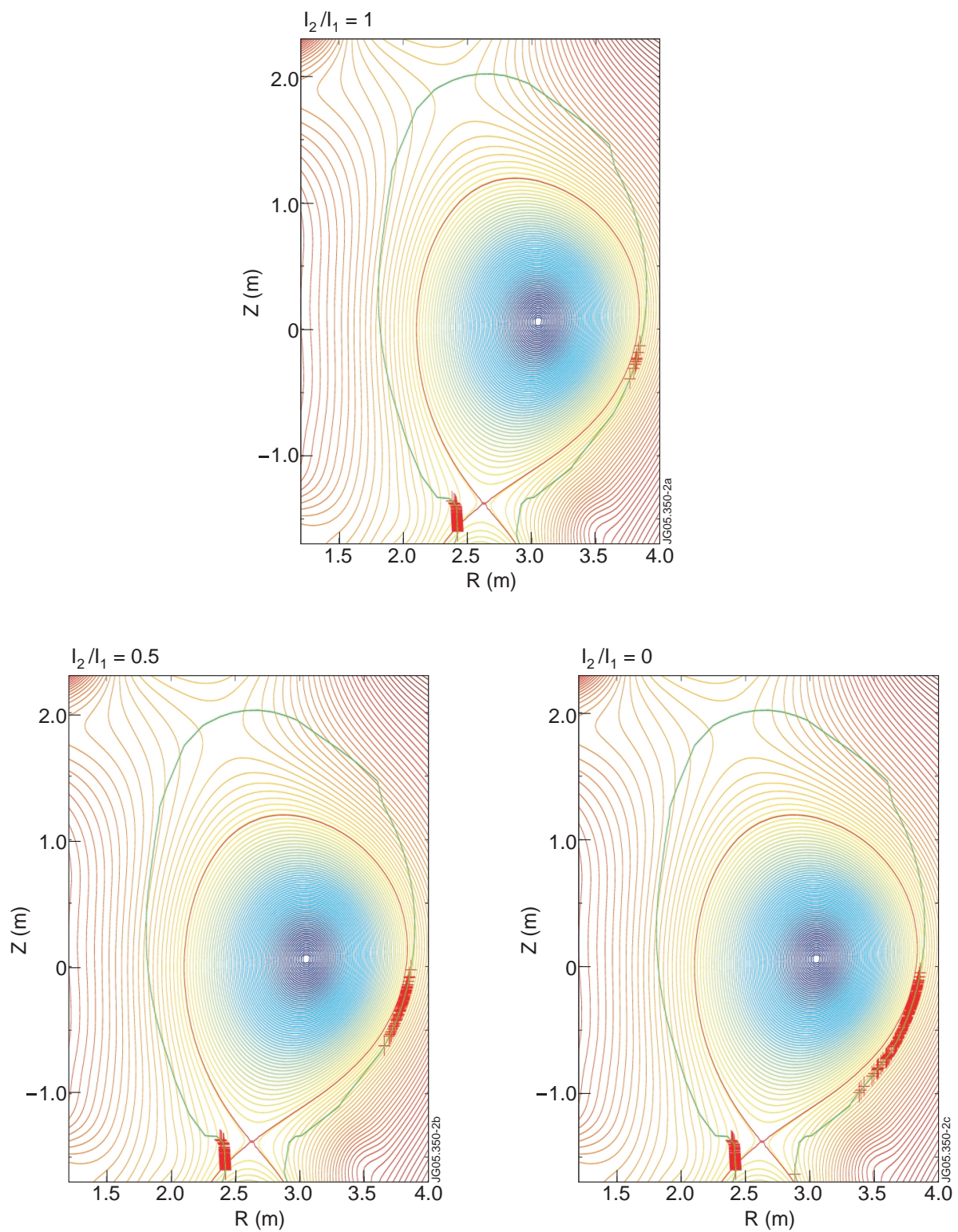


Figure 2: For larger ripple more particles are lost and loss region is wider. Here, ripple increases from left to right.

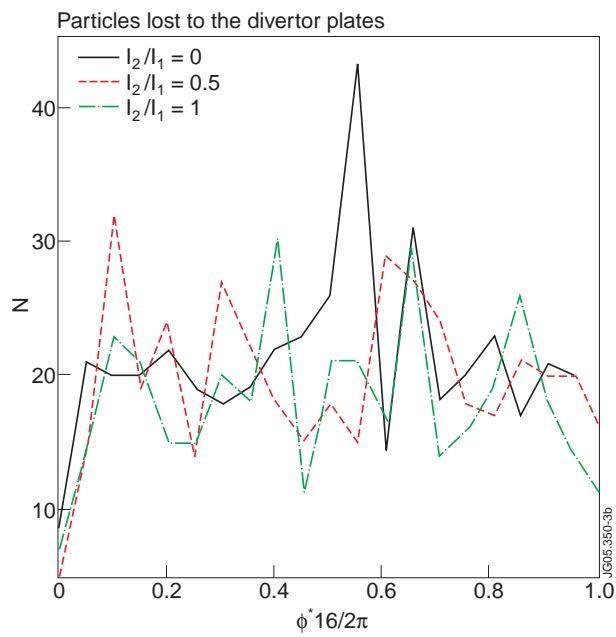
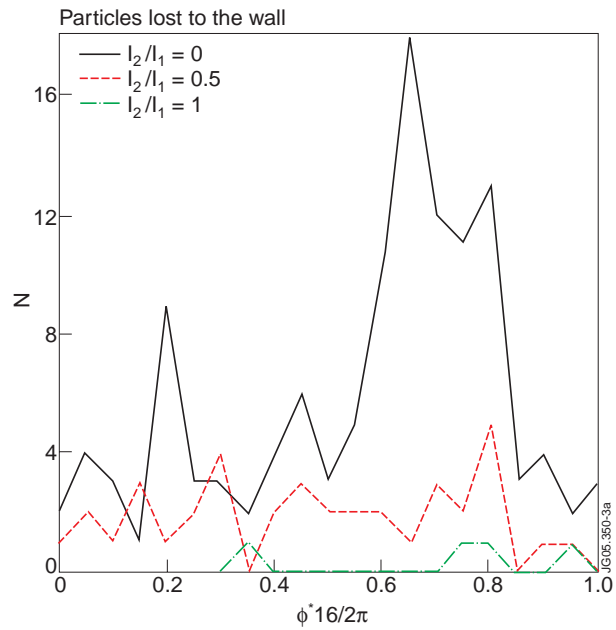


Figure 3: Number of lost test particles as a function of toroidal angle: a) Losses to the wall are localized in ϕ when ripple is large unlike losses to the divertor plates (b).